Available at
www.ElsevierComputerScience.com
POWERED BY SCIENCE DIRECT®

Computer Aided Geometric Design 21 (2004) 165–180

COMPUTER AIDED GEOMETRIC DESIGN

www.elsevier.com/locate/cagd

Interpolation with cubic spirals

Donna A. Dietz [a,*], Bruce Piper [b]

[a] *Department of Mathematics, Mansfield University, Mansfield, PA 16933, USA*
[b] *Department of Mathematical Sciences, Rensselaer Polytechnic Institute, Troy, NY 12180, USA*

Received 11 April 2003; received in revised form 14 September 2003; accepted 15 September 2003

Abstract

Numerical techniques are used to study parametric Bézier cubics of monotonic curvature, and tools are presented for design applications. Values are computed to aid in the selection of control points for building interpolatory cubic spirals, and a table is developed which helps in adjusting the endpoint curvatures.

Keywords: Monotonic curvature; Bézier cubics; Spiral

1. Introduction

While it is easy to control certain kinds of spirals (such as logarithmic spirals) simply by adjusting their equations, it is a difficult non-linear problem to control a Bézier cubic while maintaining it as a spiral. In this paper, we use numerical methods to extract information that aids in the use of cubics for applications where monotonic curvature is important. We suggest tables of values that can be used to select a particular parametric cubic spiral which interpolates given positional and tangential end conditions.

A spiral is free of local curvature extrema, making spiral design an interesting mathematical problem with importance for both physical (Gibreel et al., 1999) and aesthetic applications (Burchard et al., 1993). Since Bézier cubics are common to all modern design systems (Farin, 1996), it would be convenient to employ cubic spirals (Walton and Meek, 1996) so that spirals may be used in a variety of CAD systems.

Previous work fitting end conditions using cubics was done in several papers including (deBoor et al., 1987) upon which we build in this paper. For other work on spirals that are rational or polynomial functions and match end conditions see (Meek and Walton, 1998; Baumgarten and Farin, 1997), and (Walton and Meek, 1999) and the references therein. In (Frey and Field, 2000), the problem

* Corresponding author.
E-mail addresses: ddietzd@mansfield.edu (D.A. Dietz), piperb@rpi.edu (B. Piper).

0167-8396/$ – see front matter
doi:10.1016/j.cagd.2003.09.002

of determining which rational quadratics have monotonic curvature is shown to be tractable without numerical techniques. We incorporate many of these ideas and some from (Dietz, 2002) in the present paper.

In papers such as (Roulier et al., 1991) and (Moreton and Sequin, 1992), optimization of a "fairness measure" has been used to select free parameters in curve design. This approach works well, especially when there is an underlying physical problem that dictates a measure that leads to a unique answer. In contrast, we adopt the point of view that there is no single best answer for most problems, particularly when the primary issue in the application is visual appearance. Through the use of tables we propose a fast, simple, direct, and flexible method for meeting monotonic curvature constraints.

In the next section we develop notation used throughout the paper and present some important background results. Section 3 discusses *viable region* for cubic spirals and develops a table of values which can be used to select a cubic's inner control points so as to match given end positions and tangents. In Section 4 we develop a table for matching tangent angles as well as curvatures at the endpoints of a cubic spiral. We conclude in Section 5 with some possible applications.

2. Background and notation

Planar Bézier cubic curves are represented as

$$\mathbf{p}(t) = \sum_{\nu=0}^{3} \mathbf{b}_\nu B_\nu^3(t), \quad 0 \leqslant t \leqslant 1, \quad B_i^n(t) = \binom{n}{i} (1-t)^{n-i} t^i, \tag{1}$$

where $\mathbf{b}_0$, $\mathbf{b}_1$, $\mathbf{b}_2$, and $\mathbf{b}_3$ are control points. A complete discussion of Bézier cubics may be found in (Farin, 1996). Since it does not alter curvature properties (except by a constant scale), we will assume throughout this paper that $\mathbf{b}_0 = (0,0)$, and $\mathbf{b}_3 = (1,0)$. This leaves four degrees of freedom for design, corresponding to the control points $\mathbf{b}_1$ and $\mathbf{b}_2$ which will be assumed to lie in the fourth quadrant (so as to allow for non-negative curvature). From (1) it follows that

$$\mathbf{p}'(0) = 3(\mathbf{b}_1 - \mathbf{b}_0), \quad \mathbf{p}'(1) = 3(\mathbf{b}_3 - \mathbf{b}_2), \quad \mathbf{p}''(0) = 6(\mathbf{b}_2 - 2\mathbf{b}_1 + \mathbf{b}_0), \quad \text{and}$$
$$\mathbf{p}''(1) = 6(\mathbf{b}_3 - 2\mathbf{b}_2 + \mathbf{b}_1).$$

The tangent angle (the angle between the tangent vector and the vector $\langle 1, 0\rangle$) of the parametric cubic at $t = 0$ is denoted by ϕ_0, while the tangent angle at $t = 1$ is denoted by ϕ_1 as shown in Fig. 1.

Without loss of generality, we define spirals to be planar arcs with non-negative curvature and continuous non-zero derivative of curvature. Thus, spirals have monotonic curvature and are free from inflections but may have high winding numbers. Cubic spirals with tangent vectors that turn through smaller angles are more likely to be useful in many applications. Thus, we assume that the values for ϕ_0 and ϕ_1 are constrained so that $0 < \phi_0 < \phi_1 < \pi/2$. These constraints also restrict our search to spiral arcs of increasing curvature, as the condition $\phi_0 < \phi_1$ is necessary for this to occur (due to Vogt's theorem (Guggenheimer, 1963)). Since any spiral may be parameterized either with increasing or decreasing curvature simply by changing the direction of parameterization, arcs of increasing curvature may be studied without loss of generality.

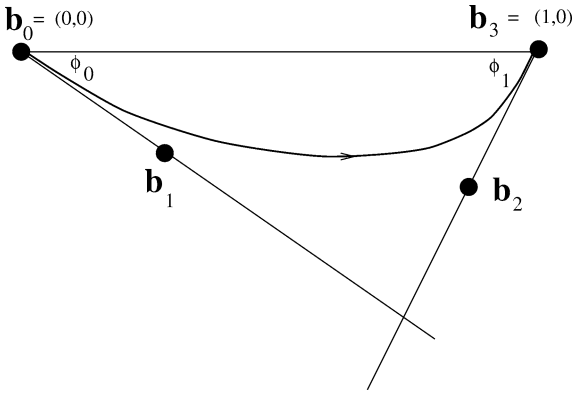

Fig. 1. Tangential conditions are specified with ϕ_0 and ϕ_1.

As shown in Fig. 1, the tangent lines for the parametric cubic at $t = 0$ and $t = 1$ and the horizontal axes form a triangle where the lengths of the lower two sides are $d_0 = \sin(\phi_1)/\sin(\phi_0 + \phi_1)$ (for the side touching the origin) and $d_1 = \sin(\phi_0)/\sin(\phi_0 + \phi_1)$. The ratios

$$f_0 = \frac{|\mathbf{b}_1 - \mathbf{b}_0|}{d_0} \quad \text{and} \quad f_1 = \frac{|\mathbf{b}_2 - \mathbf{b}_3|}{d_1} \tag{2}$$

are used extensively in this paper. To ensure the parametric cubic is free from inflections, both f_0 and f_1 are constrained to be between zero and one. This, together with the angle restrictions imposed above, implies that the cubic is convex.

Since curvature is

$$K(t) = \frac{\dot{x}\ddot{y} - \dot{y}\ddot{x}}{(\dot{x}^2 + \dot{y}^2)^{3/2}}, \tag{3}$$

the problem of designing cubic spirals could be formulated analytically as finding conditions on the (non-constant) coefficients of a fifth degree polynomial to ensure its zeros are not in $(0, 1)$. For some cubics, $\frac{dK}{dt}$ actually has five distinct real zeros.[1] Since there is no closed form for the roots of a general fifth degree polynomial, an analytic solution to this problem is not likely to be found, so we proceed numerically.

The curvatures at the endpoints of the Bézier cubic are

$$K_0 = \frac{2(\mathbf{b}_1 - \mathbf{b}_0) \wedge (\mathbf{b}_2 - 2\mathbf{b}_1 + \mathbf{b}_0)}{3|\mathbf{b}_1 - \mathbf{b}_0|^3} = \frac{1 - f_1}{f_0^2}\left(\frac{2\sin(\phi_0)\sin^2(\phi_0 + \phi_1)}{3\sin^2(\phi_1)}\right), \tag{4}$$

$$K_1 = \frac{2(\mathbf{b}_3 - \mathbf{b}_2) \wedge (\mathbf{b}_3 - 2\mathbf{b}_2 + \mathbf{b}_1)}{3|\mathbf{b}_3 - \mathbf{b}_2|^3} = \frac{1 - f_0}{f_1^2}\left(\frac{2\sin(\phi_1)\sin^2(\phi_0 + \phi_1)}{3\sin^2(\phi_0)}\right), \tag{5}$$

where $\wedge$ gives the third component of the cross product of two planar vectors.

[1] The parametric cubic $x(t) = \frac{3}{50}t^3 + \frac{1}{2}t^2 + t$, $y(t) = -\frac{19}{100}t^3 + \frac{1}{20}t^2 + t$ has this property.

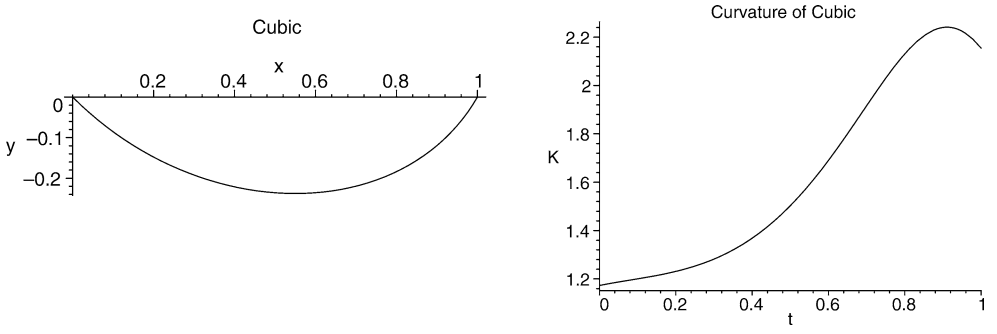

Fig. 2. Cubic satisfying $\phi_0 = \frac{\pi}{4}$, $\phi_1 = \frac{\pi}{3}$, $f_0 = 0.5$, $f_1 = 0.5$ and its curvature.

3. Suggesting f_0 and f_1 for given ϕ_0 and ϕ_1

To analyze this problem numerically, we express the four remaining degrees of freedom for parametric cubics as ϕ_0, ϕ_1, f_0, and f_1. We say that ϕ_0, ϕ_1, f_0, and f_1 *determine* a cubic since the values of $\mathbf{b}_1$ and $\mathbf{b}_2$ can be found using (2). In a context where ϕ_0 and ϕ_1 are fixed, we say that f_0 and f_1 determine a cubic.

For each given (ϕ_0, ϕ_1) pair, we define $V_f(\phi_0, \phi_1)$ to be the set of points (f_0, f_1) in $[0,1] \times [0,1]$ such that ϕ_0, ϕ_1, f_0, and f_1 determine a cubic spiral with increasing curvature. Similarly, for each given (f_0, f_1) pair, $V_\phi(f_0, f_1)$ is defined as the set of points (ϕ_0, ϕ_1) in $[0, \pi/2] \times [0, \pi/2]$ such that ϕ_0, ϕ_1, f_0, and f_1 determine a cubic spiral with increasing curvature. We shall refer to $V_f(\phi_0, \phi_1)$ and $V_\phi(f_0, f_1)$ as *viable regions*. If no confusion arises, we may just refer to a viable region without the specific notation.

For example, the cubic,

$$x(t) = .95t(1-t)^2 + 2.45t^2(1-t) + t^3, \qquad y(t) = .95t(1-t)^2 + .95t^2(1-t),$$

in which $\phi_0 = \pi/4$, $\phi_1 = \pi/3$, $f_0 = 0.5$, and $f_1 = 0.5$, is not a spiral. So, $(0.5, 0.5)$ is not in $V_f(\pi/4, \pi/3)$. Likewise, $(\pi/4, \pi/3)$ is not in $V_\phi(0.5, 0.5)$. A plot of this cubic and its curvature is shown in Fig. 2.

To reveal a viable region such as $V_f(\pi/4, \pi/3)$, we use a technique of eliminating points presented in (Frey and Field, 2000) (used in that paper to locate rational Bézier quadratics of monotone curvature). In particular, we fix $\phi_0 = \pi/4$ and $\phi_1 = \pi/3$, and for some $\tau \in [0,1]$ we use standard software to plot an implicit curve (called an *elimination curve*) in (f_0, f_1) space whose points determine cubics having $K'(\tau) = 0$. All points along an elimination curve in (f_0, f_1) space determine cubics which are not spirals, as the derivative of the curvature at τ for these points is zero. Fig. 3 shows elimination curves for various τ values between zero and one. The viable region is the remaining area; it is the set of all points in (f_0, f_1) space determining spirals for those fixed tangential end conditions. If the τ values had been sufficiently dense in $[0,1]$, the elimination curves in Fig. 3 would have completely covered the entire figure *except* for the viable region. The boundaries of the viable regions are composed of eliminations curves or (as is more common) envelopes of elimination curves.

In Fig. 4, ten viable regions, $V_f(\phi_0, \phi_1)$ are shown for various ϕ_0 and ϕ_1 values. The plot of $V_f(1.00, 1.25)$ in Fig. 4 is not sufficiently large to visually detect the viable region (which is actually non-empty in this case), so we use more accurate numerical routines. (For brevity, we omit further details.)

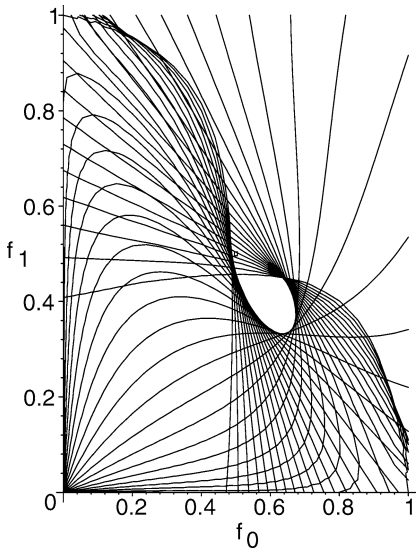

Fig. 3. Elimination curves reveal the $V_f(\pi/4, \pi/3)$ viable region.

To collect the information contained in the plots of Fig. 4, a function can be defined which maps (ϕ_0, ϕ_1) pairs to (f_0, f_1) pairs which determine cubic spirals. This is accomplished by using an interpolation scheme over an empirically derived table of (f_0, f_1) pairs such as that shown in Table 1. For this table, the (f_0, f_1) ordered pairs were chosen so that most of the table was filled by only a few such ordered pairs. For example, since the viable region $V_\phi(0.8, 0.2)$ is quite large, the ordered pair $(f_0, f_1) = (.8, .2)$ is a good ordered pair for use with many different (ϕ_0, ϕ_1) pairs. The viable regions $V_\phi(0.7, 0.5)$, $V_\phi(0.6, 0.5)$, and $V_\phi(0.6, 0.4)$ also cover many (ϕ_0, ϕ_1) pairs. Entries in Table 1 marked NVR are for (ϕ_0, ϕ_1) pairs with no associated viable regions.[2] An interpolant to the (f_0, f_1) values in Table 1 can be defined piecewise over rectangles or triangles in (ϕ_0, ϕ_1) space to produce a simple formula[3] for selecting (f_0, f_1).

While the (f_0, f_1) parameters are simple algebraically, they do not provide direct information on how to match or approximate given curvature values at the end points, and we turn our attention to this problem in the next section.

4. Suggesting ranges of K_0 and K_1 for given ϕ_0 and ϕ_1

We now consider the problem of finding useful approximations to the admissible set of endpoint curvatures of a cubic spiral. Unlike ϕ_0, ϕ_1, f_0, and f_1, which uniquely determine a cubic, the four values ϕ_0, ϕ_1, K_0, and K_1 may determine 0, 1, 2, or 3 Bézier cubics (deBoor et al., 1987). We define another type of viable region, $V_K(\phi_0, \phi_1)$, to be the set of points (K_0, K_1) with non-negative coordinates such

[2] Although another table could be created with different (f_0, f_1) values, the positions of the NVR pairs would not change.

[3] Note that the table could have been written in terms of $\cos(\phi_0)$ and $\cos(\phi_1)$ instead of ϕ_0 and ϕ_1 to avoid unnecessary calculation.

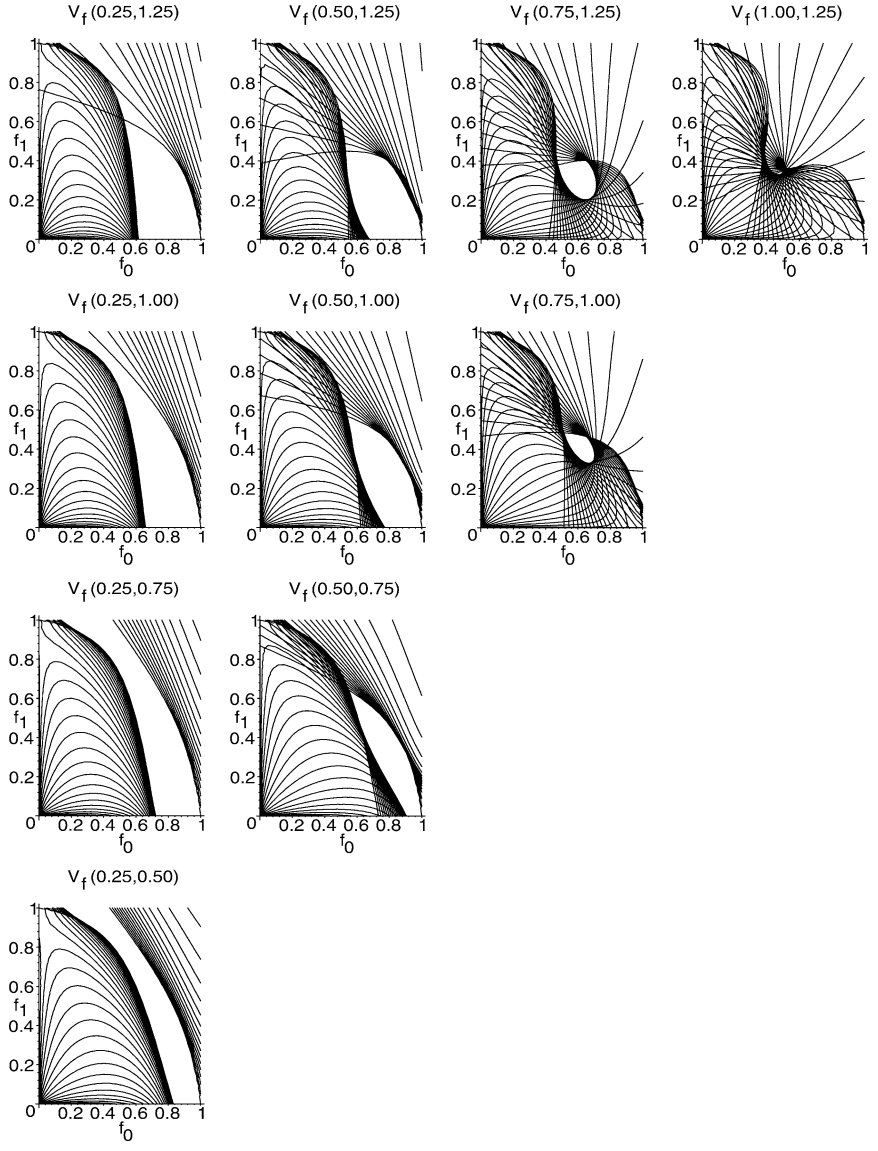

Fig. 4. $V_f(\phi_0, \phi_1)$ viable regions.

that there exists at least one cubic spiral with increasing curvature interpolating the values ϕ_0, ϕ_1, K_0, and K_1 at the ends. Although we ultimately use numerical techniques to analyze this viable region, we begin with two analytic conditions which are necessary but not sufficient for points to lie in $V_K(\phi_0, \phi_1)$.

First, for some cubic spiral to satisfy given tangential and curvature end conditions, some spiral must exist which satisfies those end conditions. From Theorem 3.18 in (Guggenheimer, 1963), there exists some convex spiral arc (not necessarily a parametric cubic) interpolating $\mathbf{b}_0$, $\mathbf{b}_3$, $\phi_0 \in (0, \pi/2)$, and $\phi_1 \in (0, \pi/2)$ with $0 < K_0 < K_1$ if and only if the circle of curvature at $\mathbf{b}_0$ contains the circle of curvature at $\mathbf{b}_3$, and $0 < \phi_0 < \phi_1 < \pi/2$. We have already imposed the latter condition by the assumptions made

Table 1
Table of f_0 and f_1 values for given ϕ_0 and ϕ_1 values

ϕ_0/ϕ_1	.2	.3	.4	.5	.6	.7	.8	.9	1.0	1.1	1.2	1.3	1.4	1.5
.1	(.8,.4)	(.8,.2)	(.8,.2)	(.8,.2)	(.8,.2)	(.8,.2)	(.8,.2)	(.8,.2)	(.8,.2)	(.8,.2)	(.8,.2)	(.8,.2)	(.8,.2)	(.8,.2)
.2		(.8,.4)	(.8,.2)	(.8,.2)	(.8,.2)	(.8,.2)	(.8,.2)	(.8,.2)	(.8,.2)	(.8,.2)	(.8,.2)	(.8,.2)	(.8,.2)	(.8,.2)
.3			(.8,.4)	(.8,.2)	(.8,.2)	(.8,.2)	(.8,.2)	(.8,.2)	(.8,.2)	(.8,.2)	(.8,.2)	(.8,.2)	(.8,.2)	(.8,.2)
.4				(.8,.4)	(.8,.2)	(.8,.2)	(.8,.2)	(.8,.2)	(.8,.2)	(.8,.2)	(.8,.2)	(.8,.2)	(.8,.2)	(.8,.2)
.5					(.8,.4)	(.8,.4)	(.8,.2)	(.8,.2)	(.8,.2)	(.8,.2)	(.8,.2)	(.8,.2)	(.8,.2)	(.8,.2)
.6						(.7,.5)	(.7,.5)	(.7,.5)	(.8,.2)	(.8,.2)	(.8,.2)	(.8,.2)	(.8,.2)	(.8,.2)
.7							(.6,.5)	(.6,.5)	(.7,.4)	(.7,.3)	(.7,.3)	(.7,.3)	(.7,.3)	(.6,.2)
.8								NVR	(.6,.4)	(.6,.4)	(.55,.35)	(.55,.3)	(.55,.3)	(.55,.25)
.9										(.5,.4)	(.5,.35)	(.5,.3)	(.5,.3)	(.45,.25)
1.0											NVR	(.45,.32)	(.43,.27)	(.42,.24)

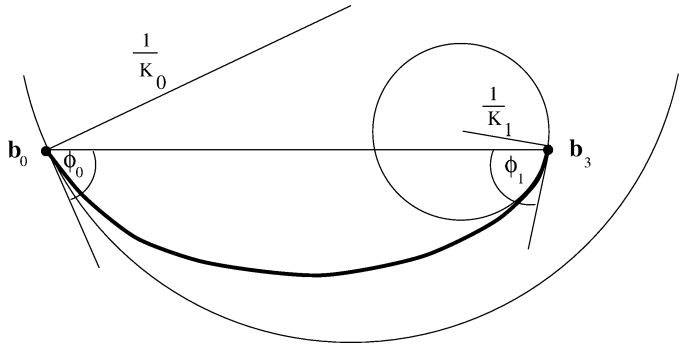

Fig. 5. Circles of curvature at $\mathbf{b}_0$ and $\mathbf{b}_3$.

in Section 2. Using elementary geometry, the former condition is formulated by imposing one constraint that is derived from the tangential contact of the two circles of curvature and a second constraint to ensure that the circle of curvature at $\mathbf{b}_0$ actually contains $\mathbf{b}_3$. (See Fig. 5.) These two constraints lead to the inequalities,

$$K_1 > \frac{2(1-\cos(\phi_0+\phi_1)) - 2K_0\sin(\phi_1)}{2\sin(\phi_0) - K_0} \quad \text{and} \quad K_0 < 2\sin(\phi_0). \tag{6}$$

When $K_0 = 0$ the condition is that the tangent line at $\mathbf{b}_0$ supports the circle of curvature at $\mathbf{b}_3$ and this again leads to the left inequality in (6). For fixed ϕ_0 and ϕ_1, the inequalities in (6) describe a region in (K_0, K_1) space above a hyperbola. (An example is shown in the right-hand plot of Fig. 7.) Points inside this region give end curvatures which can be met with an infinite number of spirals, none of which are necessarily cubics.

Second, for a cubic spiral to satisfy curvature end conditions, some parametric cubic must satisfy them. As noted previously, ϕ_0, ϕ_1, K_0, and K_1 may determine 0, 1, 2 or 3 cubics. This is shown in (deBoor et al., 1987) where results are derived on which values of K_0 and K_1 admit cubic interpolants (not necessarily spirals) for given positional and tangential end conditions. We begin with these results and give a few further details.

Eqs. (4) and (5) show the relationship between (f_0, f_1) and (K_0, K_1). To analyze this relationship for a fixed (ϕ_0, ϕ_1), let

$$\widetilde{K}_0 = \frac{1 - f_1}{f_0^2} \quad \text{and} \quad \widetilde{K}_1 = \frac{1 - f_0}{f_1^2}, \tag{7}$$

which are scaled versions of (K_0, K_1) independent of (ϕ_0, ϕ_1). The equations in (7) define a map from $(0, 1] \times (0, 1]$ in (f_0, f_1) space to $(\widetilde{K}_0, \widetilde{K}_1)$ space that is neither one to one nor onto. To discover how it folds upon itself, the singularities can be found by setting the Jacobian of this map to zero giving $-3f_1f_0 + 4f_1 + 4f_0 - 4 = 0$. This implicit curve in $(0, 1] \times (0, 1]$ can be parameterized as

$$(f_0, f_1) = \left(t, 1 - \frac{t}{4 - 3t}\right). \tag{8}$$

The image of (8) under the map defined by the equations in (7) is given by

$$\widetilde{K}_0 = \frac{1}{4t - 3t^2} \quad \text{and} \quad \widetilde{K}_1 = \frac{(4 - 3t)^2}{16(1 - t)}. \tag{9}$$

This parametric curve actually has two pre-images in $(0, 1] \times (0, 1]$. The first is, of course, the one given in (8), and the second can be found using (7) and (9) to get

$$(f_0, f_1) = \left(-t + 2\sqrt{2(t - t^2)}, \frac{4(t - 1 + \sqrt{2(t - t^2)})}{4 - 3t}\right). \tag{10}$$

In (deBoor et al., 1987), it was shown in a diagram that the curve defined by (9) and the two lines $\widetilde{K}_0 = 1$ and $\widetilde{K}_1 = 1$ divide $(\widetilde{K}_0, \widetilde{K}_1)$ space into regions with different multiplicities of solutions to prescribed curvatures at the endpoints. A similar diagram appears on the right side of Fig. 6 where points in regions *A* and *B* each have 1 corresponding cubic, points in *E* and *D* each have 2 corresponding

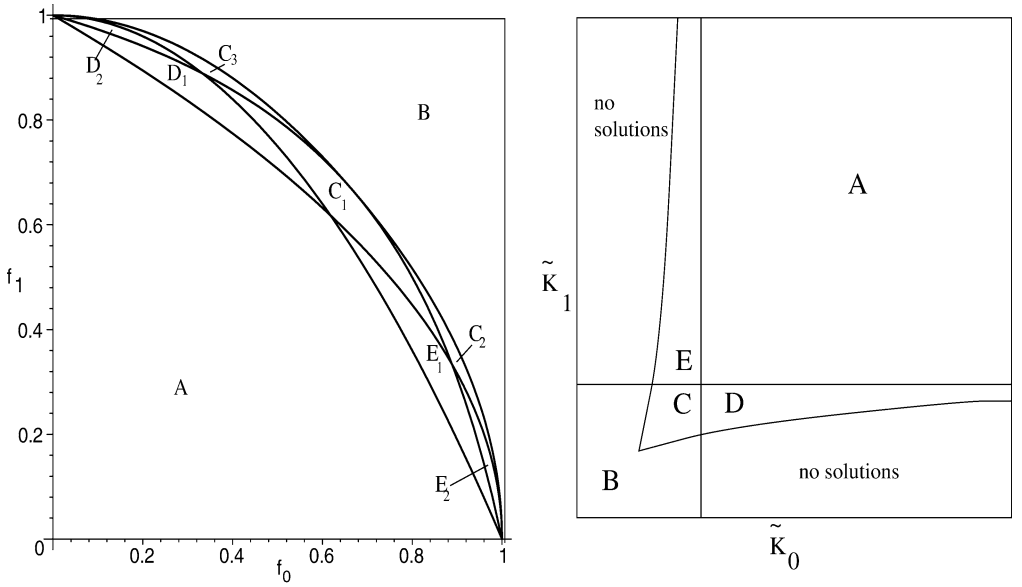

Fig. 6. Regions in (f_0, f_1) space map to regions in $(\widetilde{K}_0, \widetilde{K}_1)$ space.

cubics, and points in region C have 3 corresponding cubics. The left side of the figure illustrates the curves defined by (8) and (10) together with the pre-images of $\widetilde{K}_0 = 1$ and $\widetilde{K}_1 = 1$ under the map in (7).

These bounding curves in their respective spaces ((f_0, f_1) space and $(\widetilde{K}_0, \widetilde{K}_1)$ space) help determine which regions in each of the spaces map to each other in a one-to-one fashion. These regions are labeled in Fig. 6. Each region matches with the one(s) in the other space with the same letter. For example, the restriction of the mapping given by (7) to region C_1 in (f_0, f_1) space gives a bijection to region C in $(\widetilde{K}_0, \widetilde{K}_1)$ space. Similarly for regions C_2 and C_3, so each point of C has three corresponding pre-images in (f_0, f_1) space, one in each of the regions C_1, C_2 and C_3. Analogous statements can be made for regions D_1 and D_2 each mapping onto D and regions E_1 and E_2 each mapping onto E.

Guided by these two necessary conditions, we now turn to the numerical analysis of the sufficient conditions. We use the equations in (7) to map the elimination curves in (f_0, f_1) space into (K_0, K_1) space. This is done using standard software routines to create a piecewise linear approximation of the (implicitly defined) elimination curves and thus sequences of points which may be mapped using (7). The images are reconnected to get piecewise linear curves in (K_0, K_1) space which we call *K-elimination curves*. An example of the resulting plot superimposed with bounding curves from an unscaled version of Fig. 6 is in Fig. 7 where the lower black curve is the boundary of the region described by the inequalities in (6). The labels of the regions in Fig. 6 are used to discuss Fig. 7.

There are a few things to note in the plots in Fig. 7. The viable region, $V_K(0.2, 0.7)$, includes the white areas in regions A and B. In those regions, each point represents a unique cubic, so a single K-elimination curve through a point in regions A and B indicates that the one cubic with those ϕ_0, ϕ_1, K_0, and K_1 end conditions will not be a spiral. The $V_K(0.2, 0.7)$ viable region also contains area from region C, because

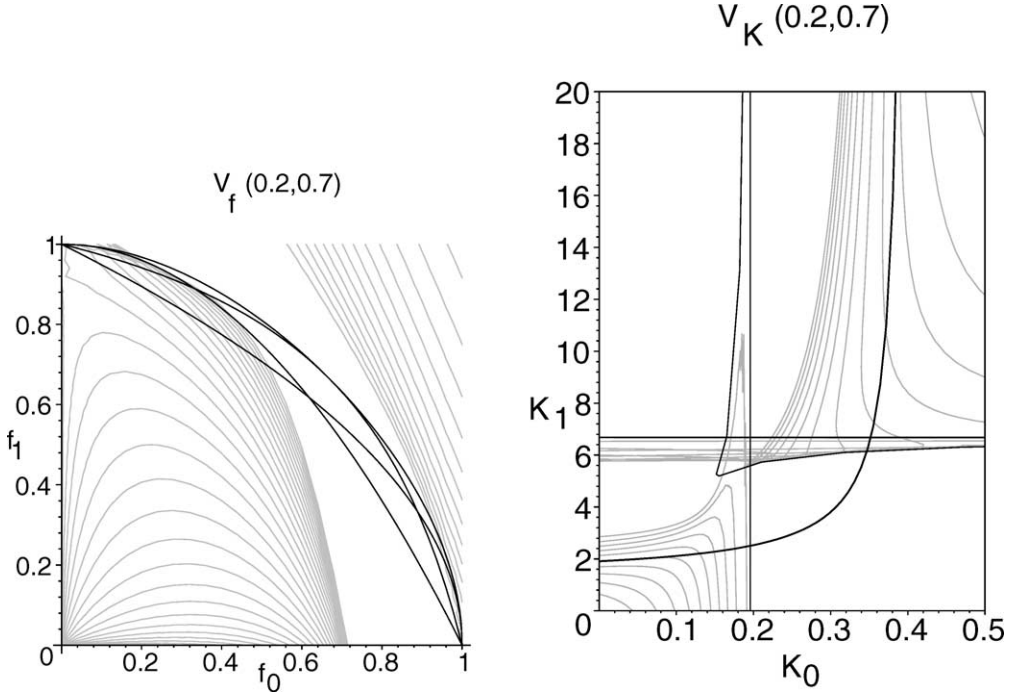

Fig. 7. Plots of $V_f(0.2, 0.7)$ and $V_K(0.2, 0.7)$.

K-elimination curves passing through C each eliminate at most one solution. Note that the region C_1 in the left plot of Fig. 7 is almost completely in $V_f(0.2, 0.7)$, therefore region C in the right plot must have pre-images in region C_1 determining cubic spirals. However, since region C_2 does have elimination curves passing through it, region C will have K-elimination curves passing through it as well even though it is in $V_K(0.2, 0.7)$. In fact, elimination curves appear in just small portions of the region C_3 in the left plot of Fig. 7, but these also show up in region C. Also, the same elimination curves which contribute just a small portion to region C_3 in the left-hand plot also contribute just a small portion to region B in the left plot near the point $(0, 1)$. Those elimination curves map to K-elimination curves in the right plot which appear as horizontal streaks near $K_1 = 6$ which pass through regions B, C, and D. A similar effect can also occur from elimination curves near $(1, 0)$ in (f_0, f_1) space.

Also, note that by (6), the end curvatures for spirals (not necessarily cubics) must lie above the lower black curve in the right plot in Fig. 7. The viable region, $V_K(0.2, 0.7)$, is a subset of the set of curvatures that correspond to any spiral, and Fig. 7 shows which portions of regions A and B are in $V_K(0.2, 0.7)$.

Thus, for each (ϕ_0, ϕ_1), plots such as those shown in Fig. 7 reveal certain parts of the viable region $V_K(\phi_0, \phi_1)$. These plots are time consuming to compute and difficult to interpret automatically. So, we proceed by creating a collection of such plots for various ϕ_0 and ϕ_1 values, extract information from each, and store it for future use.

In a design environment, it would be useful to let K_0 and K_1 vary independently. This can be accomplished if the viable region is approximated as one or more rectangles (with sides parallel to the axes) in the viable region. See Figs. 8 and 9. Of course, not all the viable region will be captured by the rectangles, but it does allow K_0 and K_1 to be chosen independently, each within specified ranges.

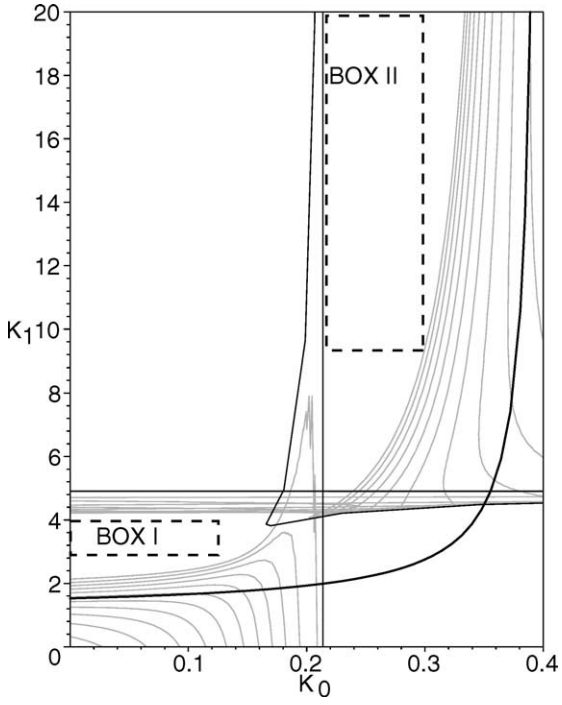

Fig. 8. Finding rectangles in $V_K(0.2, 0.6)$.

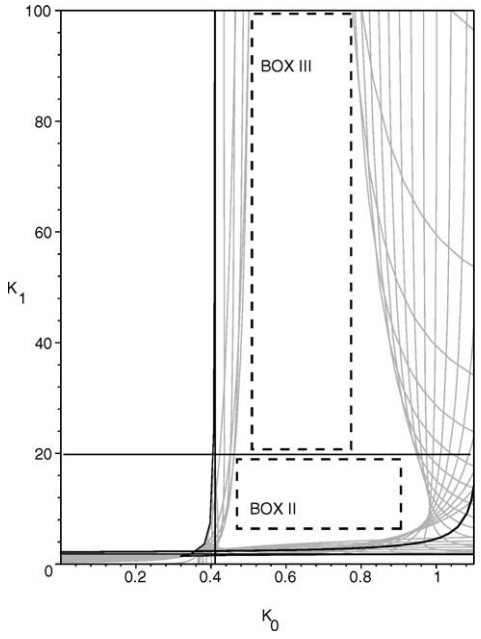

Fig. 9. Finding rectangles in $V_K(0.6, 1.2)$.

We create rectangles only in regions of (K_0, K_1) space having unique cubic solutions. The regions in (K_0, K_1) space that are omitted cause the portion of the viable region that is represented in the tables to be disconnected. The omitted region may be important for some applications, but requires considerably more rectangles and a means of identifying which of potentially several possible cubics is needed for a particular pair of curvatures. We do not pursue the problem further in the present paper.

In Table 2, three rectangles (boxes I, II, and III) are listed for each tabulated (ϕ_0, ϕ_1) pair. Absence of viable region, and hence rectangles is indicated with the letter *x*. For box I, $K_{0\min}$ is always zero. Boxes II and III lie in regions where $\widetilde{K}_0 > 1$ and $\widetilde{K}_1 > 1$, with box II not being above box III. The intent for these two rectangles is for box II to claim lower K_1 values and for box III to claim higher K_1 values. The reason for this is understood upon inspection of a typical (K_0, K_1) space viable region plot, which becomes narrower as K_1 grows. Fig. 9 is a plot of $V_K(0.6, 1.2)$. By interpolating rectangles with corresponding box numbers, the viable region for (ϕ_0, ϕ_1) values which are between tabulated values may be approximated as well. The (ϕ_0, ϕ_1) pairs from Table 1 which were marked as NVR will obviously not have boxes in Table 2. There are two additional (ϕ_0, ϕ_1) pairs, namely $(0.8, 0.9)$ and $(1.0, 1.2)$, which are not given boxes. Their viable regions, which are in region A, are only small horizontal slivers.

Since we chose to find only about 300 rectangles, each with slightly different objectives, it was simplest to suggest the rectangles manually and allow an algorithm to adjust the corners as needed. The corners of each (non-trivial) rectangle in Table 2 have been checked to ensure they lie in the viable region. The interior and the sides of each rectangle are believed to also lie in the viable region based on visual inspection of each rectangle plotted with the images of elimination curves as in Figs. 8 and 9.

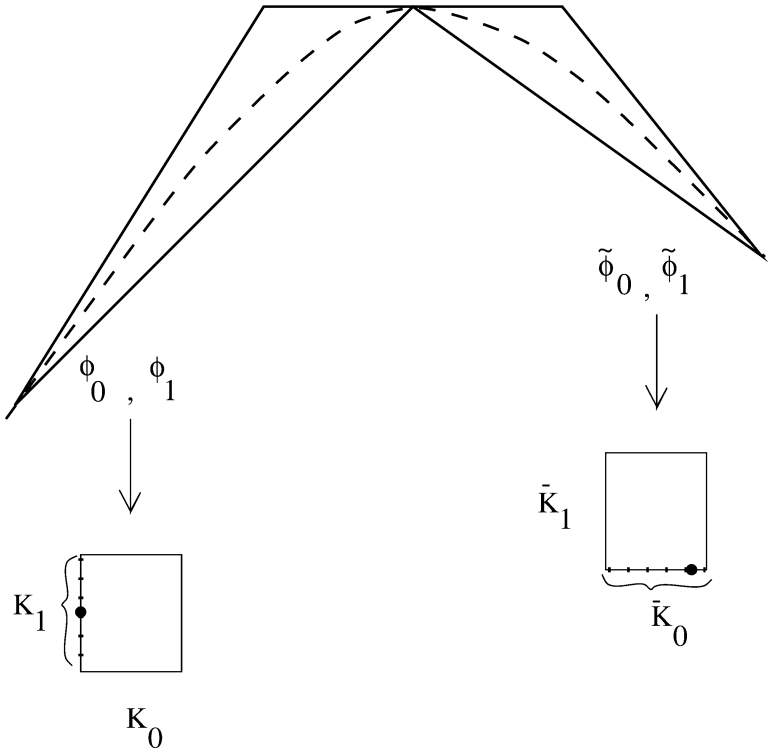

Fig. 10. A CAD system could use the tables to see if the $\overline{K}_0$ range overlaps with the K_1 range.

Table 2
Table of rectangles in (K_0, K_1) space

Angles		Box I				Box II				Box III			
		K_0		K_1		K_0		K_1		K_0		K_1	
ϕ_0	ϕ_1	min	max	min	max	min	max	min	max	min	max	min	max
.1	.2	0	.1	.72	.88	.155	.17	3	20	.16	.175	20	10^7
.1	.3	0	.075	1.6	2.23	.119	.15	7.4	18.6	.125	.165	20	10^6
.1	.4	0	.05	2.93	4.77	.101	.103	11.6	16.4	.105	.145	20	10^5
.1	.5	0	.05	4.85	7.65	.095	.12	15	20	.098	.125	20	10^5
.1	.6	0	.05	7	13	.09	.1	17	50	.095	.14	50	10^5
.1	.7	0	.05	10.9	18.1	.084	.1	29.2	44.8	.09	.13	50	9×10^4
.1	.8	0	.04	14.2	23.8	.08	.09	30	50	.08	.12	50	10^4
.1	.9	0	.04	15	20	.08	.09	38	71	.08	.12	71	10^4
.1	1	0	.03	18.2	35.8	.08	.09	46	74	.08	.11	74	10^4
.1	1.1	0	.01	20.15	41.35	.074	.09	59.6	76.4	.08	.11	82	10^4
.1	1.2	0	.04	29	48	.072	.09	64.7	78.3	.073	.1	92.2	10^3
.1	1.3	0	.04	37.7	51.3	.07	.08	63	90	.07	.1	90	10^3
.1	1.4	x	x	x	x	.07	.08	67	100	.07	.1	100	10^3
.1	1.5	x	x	x	x	.07	.072	100	100	.07	.072	100	10^3

(*continued on next page*)

Table 2 (*Continued from Table 2*)

Angles		Box I				Box II				Box III			
		K_0		K_1		K_0		K_1		K_0		K_1	
ϕ_0	ϕ_1	min	max	min	max	min	max	min	max	min	max	min	max
.2	.3	0	.2	.75	.85	.35	.37	3	20	.36	.38	20	10^4
.2	.4	0	.15	1.2	1.6	.28	.35	6	20	.3	.35	20	10^4
.2	.5	0	.1	2	2.8	.24	.32	8	20	.26	.35	20	10^4
.2	.6	0	.1	3.1	3.9	.22	.3	10	20	.225	.33	20	10^4
.2	.7	0	.1	3.8	5.4	.2	.26	11	20	.220	.31	20	10^4
.2	.8	0	.1	5.2	6.8	.188	.26	14.6	19.4	.19	.27	20	10^4
.2	.9	0	.1	6.3	8.7	.177	.24	20.5	64.5	.175	.31	70	10^4
.2	1	0	.1	8	10.4	.17	.22	17	20	.17	.31	70	10^4
.2	1.1	0	.1	9.5	12	.165	.2	16	70	.165	.3	70	10^4
.2	1.2	x	x	x	x	.15	.19	17	70	.155	.28	70	10^4
.2	1.3	x	x	x	x	.142	.15	30.6	68.4	.145	.28	81	10^4
.2	1.4	x	x	x	x	.14	.18	30	65	.14	.28	65	10^4
.2	1.5	x	x	x	x	x	x	x	x	.135	.28	85	10^4
.3	.4	0	.4	1	1	.54	.56	3	20	.55	.57	20	10^4
.3	.5	0	.3	1.4	1.5	.449	.53	5.6	18.4	.47	.52	20	10^4
.3	.6	0	.25	1.93	2.17	.38	.5	6	20	.4	.5	20	10^4
.3	.7	0	.2	2.5	2.8	.344	.47	9.2	18.8	.345	.52	20	10^4
.3	.8	0	.2	3.24	3.56	.312	.42	8.3	18.7	.315	.5	25	10^4
.3	.9	0	.15	4	4.4	.28	.4	9	20	.285	.48	20	10^4
.3	1	x	x	x	x	.26	.37	10	20	.265	.46	20	10^4
.3	1.1	x	x	x	x	.25	.38	12	20	.245	.44	20	10^4
.3	1.2	x	x	x	x	.232	.34	11.9	19.1	.235	.42	20	10^4
.3	1.3	x	x	x	x	.22	.33	13	64	.22	.48	64	10^4
.3	1.4	x	x	x	x	.2	.3	16	78	.25	.48	78	10^4
.3	1.5	x	x	x	x	.2	.28	18.5	70	.2	.48	70	10^4
.4	.5	x	x	x	x	.694	.71	5.2	16.3	x	x	x	x
.4	.6	x	x	x	x	.58	.71	3.4	20	.6	.7	20	10^4
.4	.7	x	x	x	x	.5	.7	6	20	.55	.7	20	10^4
.4	.8	x	x	x	x	.44	.63	6	20	.47	.69	20	10^4
.4	.9	x	x	x	x	.4	.62	8	20	.45	.7	20	10^4
.4	1	x	x	x	x	.37	.55	9.2	18.8	.39	.65	20	10^4
.4	1.1	x	x	x	x	.343	.55	9.2	18.8	.35	.66	20	10^4
.4	1.2	x	x	x	x	.3	.5	8	20	.33	.64	20	10^4
.4	1.3	x	x	x	x	.28	.5	10	88	.285	.66	88	10^4
.4	1.4	x	x	x	x	.265	.5	12	80	.28	.7	80	10^4
.4	1.5	x	x	x	x	.24	.45	14	20	.26	.58	20	10^4
.5	.6	x	x	x	x	.8	.86	1.6	2.2	x	x	x	x
.5	.7	x	x	x	x	.68	.78	2	20	.69	.75	20	10^4
.5	.8	x	x	x	x	.58	.8	3	20	.6	.76	20	1000
.5	.9	x	x	x	x	.53	.8	6.5	18.5	.53	.75	20	1000
.5	1	x	x	x	x	.450	.750	6	20	.470	.770	20	1000
.5	1.1	x	x	x	x	.430	.7	9.2	18.8	.410	.820	20	100
.5	1.2	x	x	x	x	.370	.750	8	20	.370	.830	20	100

(*continued on next page*)

Table 2 (*Continued from Table 2*)

Angles		Box I				Box II				Box III			
		K_0		K_1		K_0		K_1		K_0		K_1	
ϕ_0	ϕ_1	min	max	min	max	min	max	min	max	min	max	min	max
.5	1.3	x	x	x	x	.330	.7	8	20	.350	.8	20	100
.5	1.4	x	x	x	x	.3	.6	9	20	.310	.8	20	200
.5	1.5	x	x	x	x	.290	.640	11	20	.3	.8	20	200
.6	.7	x	x	x	x	.950	1	1.9	1.950	x	x	x	x
.6	.8	x	x	x	x	.750	.9	2	3.5	.770	.960	2.250	3.810
.6	.9	x	x	x	x	.650	.9	3	7.5	.660	.880	2.830	8.6
.6	1	x	x	x	x	.570	.850	4.8	16	.6	.730	16	36
.6	1.1	x	x	x	x	.510	.850	5	20	.560	.710	20	100
.6	1.2	x	x	x	x	.470	.870	6.5	20	.510	.770	20	100
.6	1.3	x	x	x	x	.450	.850	7	20	.470	.810	20	100
.6	1.4	x	x	x	x	.420	.8	7	20	.450	.840	20	100
.6	1.5	x	x	x	x	.4	.8	9	20	.450	.850	20	100
.7	.8	x	x	x	x	1.1	1.150	1.9	1.950	1.1	1.150	1.9	1.950
.7	.9	x	x	x	x	.9	1.1	2.2	3	.9	1.1	2.2	3
.7	1	x	x	x	x	.8	1	2.5	4.4	.8	1	2.5	4.4
.7	1.1	x	x	x	x	.7	1	4	6	.710	1	4	6
.7	1.2	x	x	x	x	.650	.9	4	9	.650	.9	4	9
.7	1.3	x	x	x	x	.6	.9	5	12	.6	.9	5	12
.7	1.4	x	x	x	x	.6	.750	5	20	.6	.750	5	20
.7	1.5	x	x	x	x	.560	.8	6	20	.6	.8	20	28
.8	.9	x	x	x	x	x	x	x	x	x	x	x	x
.8	1	x	x	x	x	.9	1.1	2.080	2.180	x	x	x	x
.8	1.1	x	x	x	x	.9	1.1	2.7	3.6	.9	1.1	2.6	3
.8	1.2	x	x	x	x	.8	1	3	4.8	.8	1.1	3.7	4.5
.8	1.3	x	x	x	x	.750	1.1	4	6	.8	1.1	4.1	6
.8	1.4	x	x	x	x	.7	1	5	8	.7	1	5	8
.8	1.5	x	x	x	x	.7	1	6	9	.7	1	6	9
.9	1	x	x	x	x	x	x	x	x	x	x	x	x
.9	1.1	x	x	x	x	x	x	x	x	x	x	x	x
.9	1.2	x	x	x	x	.970	1.2	2.8	3.1	x	x	x	x
.9	1.3	x	x	x	x	.9	1.1	3.2	4	x	x	x	x
.9	1.4	x	x	x	x	.8	1	3.8	4.6	.8	1	4.1	4.460
.9	1.5	x	x	x	x	.750	1	4.6	5.6	.8	1	4.840	6
1	1.1	x	x	x	x	x	x	x	x	x	x	x	x
1	1.2	x	x	x	x	x	x	x	x	x	x	x	x
1	1.3	x	x	x	x	x	x	x	x	x	x	x	x
1	1.4	x	x	x	x	1.020	1.1	3.4	3.450	x	x	x	x
1	1.5	x	x	x	x	.9	1	3.7	3.8	x	x	x	x

5. Conclusions and applications

We have presented tools that can be used to help automatically select control points for Bézier cubics. For example, the piecewise interpolant discussed in Section 3 can be used to give control points from end conditions that specify given points and tangent directions. The control points produced from the f_0 and

f_1 values are heuristically good choices in regards to monotonic curvature and if no other information or constraints are available, they could be used directly when they apply. In a design system, Table 1 could be extended to angle pairs that do not admit a spiral cubic. For such angle pairs, f_0, f_1 values would have to be chosen based on other considerations. It may actually be desirable in a design system to replace such an extended table with a more compact formula that approximates its entries, but the details of determining this table and deriving such a formula is beyond the scope of the present paper.

As an example of how a CAD system could use the information provided by Table 2, consider the following problem (Fig. 10). Given three points in $\mathbb{R}^2$ and their tangent angles, can two cubic spirals be fit with overall curvature continuity? The join point may be a local extrema of curvature (as in Fig. 10), or it may not, but in either case we wish to join two spirals with matching tangent vector and continuous (non-specified) curvature. For the two points and tangents on the left side of the figure, a linear scale (equal to the inverse of the length of the left-hand chord) is applied to each of the three boxes in Table 2 for a left (ϕ_0, ϕ_1) pair. This gives bounds on K_0 and K_1 for the left piece of the problem and similar bounds may be found for the right piece of the problem. If there is any overlap in K_1 values allowed for the left piece of the problem and K_0 values allowed for the right piece of the problem, a solution to the original problem is possible. This is shown in Fig. 10 with two (K_0, K_1) boxes. These boxes represent scaled forms of the boxes from Table 2. A join is possible if the range K_1 overlaps the range $\overline{K}_0$ and in this case, the curvatures at the outer ends, K_0 and $\overline{K}_1$, are still free to move independently in the given ranges. Since the boxes are presented for increasing curvature, different variations of the problem will require using the K_0 and K_1 from the table in the appropriate order.

The tools presented in this paper only apply to cubics, and only address the issue of monotonic curvature. Future work may try to create similar tools for other classes of curves.

Acknowledgements

The authors wish to thank the referees, whose comments helped improve this paper considerably.

References

Baumgarten, C., Farin, G., 1997. Approximation of logarithmic spirals. Computer Aided Geometric Design 14, 515–532.

Burchard, H.G., Ayers, J.A., Frey, W.H., Sapidis, N.S., 1993. Approximation with aesthetic constraints. Designing Fair Curves and Surfaces.

deBoor, C., Höllig, K., Sabin, M., 1987. High accuracy geometric Hermite interpolation. Computer Aided Geometric Design 4, 269–278.

Dietz, D.A., 2002. Convex cubic spirals. PhD Dissertation. Rensselaer Polytechnic Institute, Troy, NY.

Farin, G., 1996. Curves and Surfaces for Computer-Aided Geometric Design. Academic Press, New York.

Frey, W.H., Field, D.A., 2000. Designing Bezier conic segments with monotone curvature. Computer Aided Geometric Design 17, 457–483.

Gibreel, G.M., Easa, S.M., Hassan, Y., El-Dimeery, I.A., 1999. State of the art of highway geometric design consistency. J. Transportation Engineering 125, 305–313.

Guggenheimer, H.W., 1963. Differential Geometry. Dover, New York.

Meek, D.S., Walton, D.J., 1998. Planar spirals that match G^2 hermite data. Computer Aided Geometric Design 15, 103–126.

Moreton, H.P., Sequin, C.H., 1992. Functional optimization for fair surface design. In: SIGGRAPH'92 Proceedings, pp. 167–176.

Roulier, J.A., Rando, T., Piper, B., 1991. Fairness and monotonic curvature. In: Chui, C. (Ed.), Approximation Theory and Functional Analysis. Academic Press.

Walton, D.J., Meek, D.S., 1996. A planar cubic Bézier spiral. J. Comput. Appl. Math. 72, 85–100.

Walton, D.J., Meek, D.S., 1999. Planar G^2 transition between two circles with a fair cubic Bézier curve. Computer-Aided Design 31, 857–866.